THE JOURNAL OF BIOLOGICAL CHEMISTRY VOL. 291, NO. 24, pp. 12888–12896, June 10, 2016

Direct Demonstration That Loop1 of Scap Binds to Loop7

*A CRUCIAL EVENT IN CHOLESTEROL HOMEOSTASIS**

Received for publication, March 28, 2016, and in revised form, April 8, 2016 Published, JBC Papers in Press, April 11, 2016, DOI 10.1074/jbc.M116.729798

Yinxin Zhang[‡1], Kwang Min Lee[‡2], Lisa N. Kinch[§], Lindsay Clark[¶], Nick V. Grishin[§¶‖], Daniel M. Rosenbaum[¶‖], Michael S. Brown[‡3], Joseph L. Goldstein[‡4], and Arun Radhakrishnan[‡5]

From the Departments of [‡]Molecular Genetics, [¶]Biophysics, and [‖]Biochemistry and [§]Howard Hughes Medical Institute, University of Texas Southwestern Medical Center, Dallas, Texas 75390

Cholesterol homeostasis is mediated by Scap, a polytopic endoplasmic reticulum (ER) protein that transports sterol regulatory element-binding proteins from the ER to Golgi, where they are processed to forms that activate cholesterol synthesis. Scap has eight transmembrane helices and two large luminal loops, designated Loop1 and Loop7. We earlier provided indirect evidence that Loop1 binds to Loop7, allowing Scap to bind COPII proteins for transport in coated vesicles. When ER cholesterol rises, it binds to Loop1. We hypothesized that this causes dissociation from Loop7, abrogating COPII binding. Here we demonstrate direct binding of the two loops when expressed as isolated fragments or as a fusion protein. Expressed alone, Loop1 remained intracellular and membrane-bound. When Loop7 was co-expressed, it bound to Loop1, and the soluble complex was secreted. A Loop1-Loop7 fusion protein was also secreted, and the two loops remained bound when the linker between them was cleaved by a protease. Point mutations that disrupt the Loop1-Loop7 interaction prevented secretion of the Loop1-Loop7 fusion protein. These data provide direct documentation of intramolecular Loop1-Loop7 binding, a central event in cholesterol homeostasis.

A vast assortment of lipids populates the membranes of mammalian cells. For membranes to function optimally, the amounts of these lipids must be carefully controlled, but the control mechanisms are poorly understood. Recent progress has been made in understanding the machinery that controls one such lipid, *i.e.* cholesterol. The central player is a cholesterol-binding membrane protein, Scap, that mediates feedback inhibition of sterol regulatory element-binding proteins (SREBPs),[6] transcription factors that activate cholesterol synthesis (1).

SREBPs are synthesized as intrinsic proteins of endoplasmic reticulum (ER) membranes. Immediately after synthesis, SREPBs bind to Scap. The Scap-SREBP complex is incorporated into vesicles that move to the Golgi, where the SREBPs are processed by two proteases that liberate the transcriptionally active fragment (2). This fragment enters the nucleus, where it activates transcription of all genes whose products are required for cholesterol synthesis (3). When cholesterol levels in ER membranes rise above 5% of total lipids, the Scap-SREBP complex binds to Insig, an ER anchor protein that prevents export to the Golgi (4). SREBPs are no longer processed, and cholesterol synthesis declines. This end product feedback mechanism assures that cells provide themselves with the cholesterol they need for membrane function while avoiding toxic cholesterol overaccumulation.

In recent years, our laboratory has performed a molecular dissection of Scap, identifying the domains responsible for each of its functions (5–7). Our current working model is shown in Fig. 1. All of the sterol regulation is confined to the membrane portion of Scap, which contains eight transmembrane helices. The eight helices are connected by three large loops (1, 6, and 7) and four small loops (2–5) (Ref. 8). Loop1 (L1) projects into the ER lumen. When produced as a fragment by recombinant DNA methods, L1 behaves as a membrane-anchored protein, requiring detergents for solubilization. It binds cholesterol and other sterols with a specificity that matches the specificity defined previously for the entire membrane domain of Scap (6, 9). Based on indirect evidence, we proposed that L1 binds to Loop7 (L7), the other large intraluminal loop (7). The interaction of L1 with L7 maintains cytosolic Loop6 in a conformation that allows the binding of COPII proteins that cluster the Scap-SREBP complex into coated vesicles for transit to the Golgi. The COPII proteins bind to MELADL, a hexapeptide in Loop6 (5). When ER cholesterol rises above a threshold of 5 mol% of total lipids, cholesterol binds to L1, producing a conformational change in

* This work was supported by National Institutes of Health Grants GM HL20948 (to J. L. G. and M. S. B.), GM094575 (to N. V. G.), and R01GM113050 (to D. M. R.); Robert A. Welch Foundation Grants I-1793 (to A. R.), I-1505 (to N. V. G.), and I-1770 (to D. M. R.); and American Heart Association Grants 12SDG12040267 (to A. R.) and 16PRE27200004 (to L. C.). The authors declare that they have no conflicts of interest with the contents of this article. The content is solely the responsibility of the authors and does not necessarily represent the official views of the National Institutes of Health.

[1] Present address: Laboratory of Molecular Genetics and Howard Hughes Medical Institute, The Rockefeller University, New York, NY 10065.

[2] Present address: Korea Food Research Institute, Seongnam-si, Gyeonggi-do 13539, Republic of Korea.

[3] To whom correspondence may be addressed: Dept. of Molecular Genetics, University of Texas Southwestern Medical Center, 5323 Harry Hines Blvd., Dallas, TX 75390-9046. Tel.: 214-648-2179; Fax: 214-648-8804; E-mail: mike.brown@utsouthwestern.edu.

[4] To whom correspondence may be addressed: Dept. of Molecular Genetics, University of Texas Southwestern Medical Center, 5323 Harry Hines Blvd., Dallas, TX 75390-9046. Tel.: 214-648-2141; Fax: 214-648-8804; E-mail: joe.goldstein@utsouthwestern.edu.

[5] To whom correspondence may be addressed: Dept. of Molecular Genetics, University of Texas Southwestern Medical Center, 5323 Harry Hines Blvd., Dallas, TX 75390-9046. Tel.: 214-648-0329; Fax: 214-648-8804; E-mail: arun.radhakrishnan@utsouthwestern.edu.

[6] The abbreviations used are: SREBP, sterol regulatory element-binding protein; ER, endoplasmic reticulum; L1, Loop1; L7, Loop7; MCD, methyl-β-cyclodextrin; Ni^{2+}-NTA, nickel-nitrilotriacetic acid; aa, amino acids; TEV, tobacco etch virus; PNGase F, peptide-*N*-glycosidase F; NP40, Nonidet P-40.

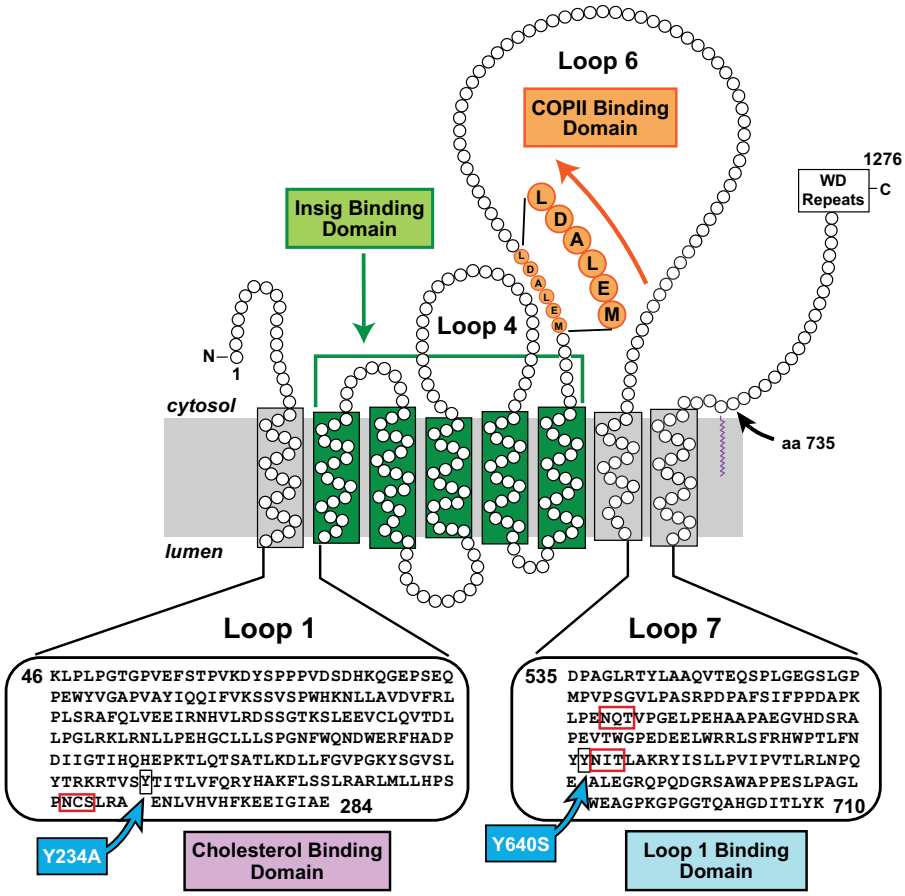

FIGURE 1. **Model illustrating the functional domains of Scap.** The membrane-bound portion of hamster Scap (amino acids 1–753) includes four functional domains. Luminal L1 (amino acids 46–284) binds cholesterol. This domain contains a glycosylation site (*red box*) and a tyrosine residue (Tyr-234) that, when mutated to alanine, renders Scap unable to move to the Golgi (6). Transmembrane helices 2–6 (*green*) contain the Insig-binding domain. Cytoplasmic Loop6 contains the hexapeptide MELADL (*orange*) that binds to COPII proteins (10). Luminal L7 (amino acids 535–710) binds to luminal L1. This domain contains two glycosylation sites (*red boxes*) and a tyrosine residue (Tyr-640) that, when mutated to serine, renders Scap unable to move to the Golgi (7).

Loop6 that renders MELADL inaccessible to COPII proteins (10). We have indirect evidence that cholesterol binding causes L1 to dissociate from L7 and that this causes the conformational change in Loop6 (7). The cholesterol-induced conformational change also causes Scap to bind to Insig, which interacts with the Insig-binding domain, a cluster of five transmembrane helices (helices 2–6) (1). Evidence suggests that point mutations in either L1 (Y234A) or L7 (Y640S) disrupt the binding of Loops1 and 7, locking Scap into its cholesterol-bound conformation, increasing the interaction with Insig and preventing COPII binding to Loop6 even when membrane cholesterol levels are low (6, 7). So far, however, the inference that Scap L1 binds to L7 has been indirect.

In this study, we demonstrate a direct interaction between L1 and L7 using soluble protein complexes that are secreted when the two loops are produced together in transfected cells or when the two loops are expressed as a fusion protein. The results provide crucial insights into the structural basis for this interaction.

Experimental Procedures

Reagents—We obtained [1,2,6,7-^{3}H]cholesterol (100 Ci/mmol) from American Radiolabeled Chemicals (St. Louis, MO); cholesterol and DTT from Sigma; desmosterol, 25-hydroxycholesterol, and epicholesterol from Steraloids, Inc. (Newport, RI); Cellgro ITS and AcTEV protease from Fisher Scientific (Waltham, MA); hydroxypropyl cyclodextrin and methyl-β-cyclodextrin (MCD) from Cyclodextrin Technologies (Gainesville, FL); PNGase F from New England Biolabs (Ipswich, MA); Fos Choline 13 (FC13), octylglucoside, and CHAPS from Anatrace (Maumee, OH); Nonidet P-40 (NP40) detergent from Roche Applied Sciences; Ni^{2+}-NTA-agarose beads from Qiagen (Hilden, Germany); mouse monoclonal anti-His antibody and Superdex 200 10/300 GL columns from GE Healthcare; gel filtration standards from Bio-Rad; and centrifugal filter units from Millipore (Billerica, MA). Rabbit β-VLDL (density $<$ 1.006 g/ml) was prepared by ultracentrifugation (11).

Monoclonal Antibodies—IgG-9D5, a mouse monoclonal antibody against hamster Scap (amino acids 540–707), hereafter designated anti-L7, has been described previously (12). The monoclonal antibody IgG-7G5 against hamster SCAP was produced by immunizing BALB/c mice with a fusion protein encoding a hexahistidine epitope tag followed by amino acids (aa) 46–269 of hamster Scap (6) and subsequent screening of hybridoma clones by ELISA. One positive hybridoma (IgG-7G5) was subcloned by serial dilution three times and purified

by affinity chromatography on protein G-Sepharose 4 Fast Flow columns. We hereafter refer to IgG-7G5 as anti-L1.

Buffers and Media—Buffer A contained 50 mM Tris-chloride (pH 7.4) and 150 mM NaCl. Buffer B contained 10 mM Tris-chloride (pH 7.4), 100 mM NaCl, and 1% SDS. Medium A contained a 1:1 mixture of Ham's F-12 and Dulbecco's modified Eagle's medium (Mediatech, Inc.) supplemented with 100 units/ml penicillin and 100 μg/ml streptomycin sulfate.

Plasmids—An expression vector encoding wild-type hamster Scap under the control of the CMV promoter (12) was modified by site-directed mutagenesis to generate three expression plasmids: pCMV-Scap-L1, pCMV-Scap-L7, and pCMV-Scap(L1-L7). pCMV-Scap-L1 and pCMV-Scap-L7 encode, in sequential order from the NH_2 terminus, the 24-aa signal sequence from human Niemann-Pick C1 (NPC1) (13) and either luminal L1 of Scap (aa 47–269) followed by a FLAG epitope tag (DYKDDDDK) or luminal L7 of Scap (aa 538–710), respectively (Fig. 1). pCMV-His_{12}-Scap(L1-L7) encodes, in sequential order from the NH_2 terminus, the 24-aa signal sequence from human NPC1, an epitope tag consisting of 12 histidines, luminal Loop1 of Scap (aa 46–284), a 15-aa linker that includes a TEV protease cleavage site (SENLYFQGSSGSSGS) (14), and luminal Loop7 of Scap (aa 535–710).

A pFastBacHTa expression vector (Life Technologies) encoding amino acids 1–767 of hamster Scap (15) was modified by site-directed mutagenesis (QuikChange II XL kit, Stratagene) to generate three recombinant baculoviruses designated pBac-His_6-Scap-L1, pBac-His_{10}-Scap-L7, and pBac-His_{10}-Scap(L1-L7). pBac-His_6-Scap-L1 and pBac-His_{10}-Scap-L7 encode, in sequential order from the NH_2 terminus, the 21-aa signal sequence from honeybee mellitin, a 4-aa linker (DSYY), an epitope tag consisting of six or 10 histidines, a 17-aa linker that includes a TEV protease cleavage site (DYDIPTTENLYFQGAMG), and luminal L1 of Scap (aa 46–269) or luminal L7 of Scap (aa 538–710). pBac-His_{10}-Scap(L1-L7) encodes, in sequential order from the NH_2 terminus, the 21-aa signal sequence from honeybee mellitin, a 4-aa linker (DSYY), an epitope tag consisting of 10 histidines, a 10-aa linker (DYDIPTTAMG), luminal L1 of Scap (aa 46–284), a 15-aa linker that includes the TEV protease cleavage site (see above), and luminal L7 of Scap (aa 535–710). Point mutations in the above Scap plasmids were generated by site-directed mutagenesis, and mutations were verified by sequencing the entire coding region of all plasmids.

Cell Culture—Hamster CHO-K1 cells were grown in monolayer at 37 °C and 8–9% CO_2 in medium A supplemented with 5% FCS. The protocol for transfecting cDNAs into CHO-K1 cells is described in the figure legends.

Purification of His-tagged Scap(L1-L7) from Sf9 Media—On day 0, 1-liter cultures of Sf9 (10^6 cells/ml) in Sf-900 II SFM insect medium (Invitrogen) were set up at 27 °C. On day 1, cells were infected with the pBac-His_{10}-Scap(L1-L7) baculovirus. On day 3, cells were harvested and washed once with PBS. The cells were then flash-frozen in liquid nitrogen and stored at −80 °C. The Sf-900 II SFM insect medium containing secreted His_{10}-Scap(L1-L7) was loaded onto a 5-ml Ni^{2+}-NTA-agarose column equilibrated with 10 column volumes of buffer A and then washed sequentially with 10 column volumes each of buffer A containing 20 mM imidazole and 40 mM imidazole. Bound proteins were eluted with 10 column volumes of buffer A containing 200 mM imidazole. The eluates were pooled, concentrated with a Millipore centrifugal filter unit (30,000 molecular weight cutoff) to 0.5 ml, and then applied to a Superdex 200 10/300 GL column that had been pre-equilibrated with buffer A. Fractions containing His_{10}-Scap(L1-L7) were combined, concentrated, stored at 4 °C, and designated as purified His_{10}-Scap(L1-L7). The purified protein was used for assays within 4 days.

Immunoprecipitation of Scap—In experiments with transfected cells, medium containing secreted proteins was subjected to $10^5 \times g$ centrifugation, and the supernatants were incubated with 1 μg/ml anti-L7 or control mouse monoclonal antibody. After 1 h, 100 μl of protein A/G Plus-agarose beads (Santa Cruz Biotechnology, Dallas, TX) was added, followed by overnight incubation on a rotator and centrifugation at 1000 × *g* for 10 min. In experiments with purified His_{10}-Scap(L1-L7), reaction mixtures were incubated with 50 μl of protein A/G Plus-agarose beads along with 1 μg/ml anti-L1 or control mouse monoclonal antibody. After incubation at room temperature for 40 min, the reactions were centrifuged at 2000 × *g* for 2 min. In both types of experiments, the resulting supernatants were transferred to a fresh tube and designated as the supernatant. The pelleted beads were washed three times with 1 ml of buffer A, resuspended in 1 ml of buffer B, and heated at 95 °C for 10 min. The mixtures were clarified by centrifugation at 1000 × *g* for 5 min, and the resulting fractions were designated as the pellet. Equivalent fractions of supernatants and pellets were subjected to immunoblot analysis.

[^{3}H]Cholesterol-binding Assay—Binding assays were carried out as described previously (6). Each reaction, in a final volume of 100 μl of buffer A with 0.004% (w/v) NP40 and 0.002% (w/v) FC13, contained 2 pmol (140 ng) of purified His_{10}-Scap(L1-L7) and the indicated concentration of [^{3}H]cholesterol (delivered in 2.5 μl of ethanol) in the absence or presence of competitor sterol (delivered in 1 μl of ethanol). After incubation for 4 h at room temperature, each reaction was loaded onto a column packed with 0.3 ml of Ni^{2+}-NTA-agarose beads pre-equilibrated with 2 ml of buffer A. The columns were washed with 5 ml of buffer A and then eluted with 1 ml of the same buffer containing 250 mM imidazole. Aliquots of the eluate (0.7 ml) were assayed for radioactivity in a liquid scintillation counter.

Immunoblot Analysis—Samples for immunoblotting were subjected to 8% or 13% SDS-PAGE, after which the proteins were transferred to nitrocellulose filters that were incubated at room temperature for 1 h with primary antibodies as indicated in the figure legends. Bound antibodies were visualized by chemiluminescence (SuperSignal West Pico chemiluminescent substrate, Thermo Scientific) using a 1:5000 dilution of mouse IgG TrueBlot® Ultra (Rockland Immunochemicals Inc.) conjugated to horseradish peroxidase. Immunoblots were exposed to Phoenix Research Products Blue x-ray film (F-BX810) at room temperature. Films were exposed for 1–20 s.

Reproducibility—Similar results were obtained when each experiment was independently repeated on three or more occasions.

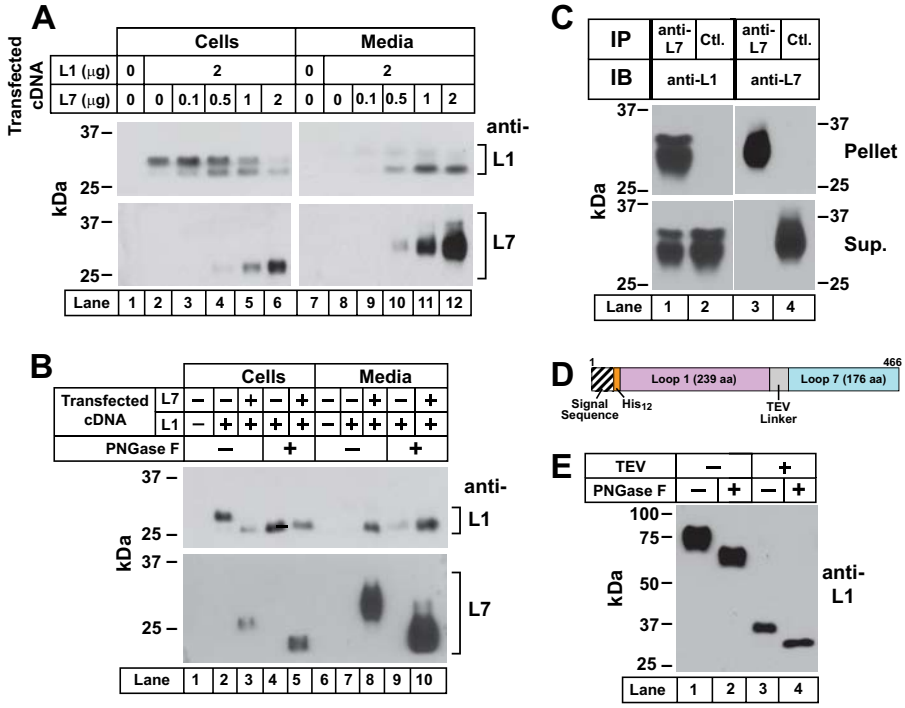

FIGURE 2. **Secretion of L1 by CHO-K1 cells requires interaction with L7.** *A–C*, on day 0, CHO-K1 cells were set up for experiments in 3 ml of medium A containing 5% FCS at a density of 6×10^5 cells/60-mm dish. On day 1, cells were switched to 3 ml of medium A containing 1% ITS and co-transfected with the indicated cDNAs as described below. FuGENE 6 was used as the transfection agent according to the instructions of the manufacturer. The total amount of DNA was adjusted to 4 μg/dish by addition of pcDNA empty vector. On day 3, medium was collected from each group (2 dishes/condition) and pooled (6 ml total), and the cells from each group were harvested, pooled, and resuspended in PBS (1 ml total). *A*, transfection with the indicated amounts of pCMV-Scap-L1 and pCMV-Scap-L7. After transfection, equivalent fractions of cells and medium (0.6% of total) were subjected to immunoblot analysis with 5 μg/ml anti-L1 or 0.5 μg/ml anti-L7. *B*, transfection with 2 μg of pCMV-Scap-L1 plus 2 μg of pCMV-Scap-L7. After transfection, aliquots of cells and media (5% of total) were subjected to glycolytic digestion by PNGase F according to the instructions of the manufacturer and processed for immunoblot analysis as above. *C*, transfection as above. After transfection, aliquots of the pooled media (1 ml) were centrifuged at $10^5 \times g$, and the supernatants were subjected to immunoprecipitation (*IP*) with 1 μg/ml anti-L7 (*lanes 1* and *3*) or control monoclonal antibody (*lanes 2* and *4*) as described under "Experimental Procedures." Equivalent fractions of immunoprecipitated pellets and supernatants (2% of total) were subjected to immunoblot analysis (*IB*) with 1 μg/ml anti-L1 (*lanes 1* and *2*) or 5 μg/ml anti-L7 (*lanes 3* and *4*). *D*, schematic of recombinant L1-L7 secreted by CHO-K1 cells. Starting at the NH_2 terminus, the construct contains the NPC1 signal sequence (*black* and *white stripes*), followed by a His_{12} epitope tag (*brown*), hamster Scap-L1 (aa 46–284, *pink*), a TEV protease site (*gray*), and hamster Scap-L7 (aa 535–710, *blue*). *E*, transfection with 4 μg of pCMV-His_{12}-Scap(L1-L7) as above. After transfection, aliquots of the pooled media (2 ml) were passed over a 1-ml nickel column that was pre-equilibrated with buffer A. After washing with 10 ml of buffer A containing 50 mM imidazole, His_{12}-Scap(L1-L7) was eluted with 2 ml of buffer A containing 200 mM imidazole. Each reaction, in a final volume of 100 μl, contained 50 μl of purified His_{12}-Scap(L1-L7) without or with 10 units of TEV protease. After incubation for 3 h at room temperature, aliquots of each reaction (50% of total) were subjected to glycolytic digestion by PNGase F and processed for immunoblot analysis with 5 μg/ml anti-L1. *Sup*, supernatant; *Ctl*, control.

Results

To facilitate studies of the L1/L7 interaction, we prepared expression plasmids encoding L1 or L7, both of which were preceded by a signal sequence from human NPC1. When transfected into CHO-K1 cells and analyzed by SDS-PAGE, L1 was expressed as a single species that was retained in cells and not secreted into the medium (Fig. 2*A*, *top lanes 2* and *8*). A similar observation was made previously in insect cells, where a baculovirus encoding L1 produced a membrane-attached protein that was retained in the cell and required detergents for solubilization (6). When we used transfection to produce increasing amounts of L7 together with L1, the CHO-K1 cells contained an additional species of L1 that migrated faster on SDS-PAGE (Fig. 2*A*, *top lanes 3–6*). When the amount of L7 plasmid was raised, most of this faster-migrating L1 was found in the medium (Fig. 2*A*, *top lanes 10–12*) together with the majority of L7 (Fig. 2*A*, *bottom lanes 10–12*). A small fraction of L7 was retained in the cells (Fig. 2*A*, *bottom lanes 5* and *6*). This retained L7 migrated more rapidly than the secreted protein.

Because L1 and L7 contain one and two potential *N*-linked glycosylation sites, respectively (Fig. 1), we tested whether the different species of L1 and L7 were products of differential glycosylation. CHO-K1 cells were transfected with plasmids producing L1 alone or with L1 plus L7. Cell lysates and media were treated with peptide-*N*-glycosidase F (PNGase F). Again, singly transfected L1 was retained in cells (Fig. 2*B*, *top lanes 2* and *7*). Treatment of the retained L1 with PNGase F reduced its apparent mass in a single step (Fig. 2*B*, *top lanes 2* and *4*), indicating that its sole *N*-linked glycosylation site sequence (NCS) was glycosylated. When L7 was expressed concurrently with L1, L1 was no longer glycosylated, and the unglycosylated protein was secreted into the medium, where its size was no longer reduced by PNGase F treatment (Fig. 2*B*, *top lanes 3*, *5*, *8*, and *10*). On the other hand, intracellular and secreted L7 continued to be glycosylated because treatment with PNGase reduced the molecular weights of both forms of L7 (Fig. 2*B*, *bottom lanes 3*, *5*, *8*, and *10*).

We next conducted co-immunoprecipitation assays to determine whether L7 facilitates the solubilization and secretion of L1 by a direct interaction (Fig. 2*C*). For these assays, CHO-K1 cells were transfected with plasmids encoding L1 plus L7. The medium containing secreted proteins was subjected to centrif-

ugation at $10^5 \times g$ to eliminate insoluble materials. We incubated the $10^5 \times g$ supernatant with a monoclonal antibody to L7 and captured the antibody-bound protein on protein A/G-agarose beads. The proteins that did not adhere to the beads (designated supernatant) and the proteins eluted from the pelleted beads (designated pellet) were subjected to SDS-PAGE and immunoblot analysis. As shown in Fig. 2*C*, both secreted L1 and L7 were precipitated by anti-L7 (*lanes 1* and *3*) but not by a control antibody (*lanes 2* and *4*). Densitometric analysis of the data in Fig. 2*C* and two other co-immunoprecipitation experiments showed that 40–70% of secreted L1 was co-immunoprecipitated with L7.

To further study the glycosylation status of L1 when it is bound to L7, we prepared a plasmid that encodes L1 followed by L7 separated by a 15-amino acid linker containing a TEV protease cleavage site (Fig. 2*D*). This plasmid was preceded by a signal sequence from human NPC1 followed by 12 histidine residues. We refer to this fusion protein as L1-L7. We transfected CHO-K1 cells with the L1-L7 plasmid, and the secreted L1-L7 was purified by nickel chromatography. Treatment of purified L1-L7 with PNGase F reduced its apparent molecular weight (Fig. 2*E*, *lanes 1* and *2*), indicating that one or more of the three *N*-linked glycosylation site sequences in L1-L7 was glycosylated. To determine the glycosylation status of L1 in this fusion protein, we first digested purified L1-L7 with TEV protease. Treatment of the liberated L1 with PNGase F reduced its apparent molecular weight in a single step (Fig. 2*E*, *lanes 3* and *4*), indicating that the sole *N*-linked site in L1 was glycosylated when it was fused to L7. For an interpretation of these results, see "Discussion."

We next sought to determine whether formation of the L1-L7 complex in transfected cells is regulated by cholesterol. CHO cells were transfected with plasmids encoding L1 and L7 and then depleted of cholesterol by incubation with hydroxypropyl cyclodextrin, followed by incubation with no sterol, cholesterol, or epicholesterol, delivered in complex with MCD (9, 16). Cells and medium were subjected to SDS-PAGE and blotted with anti-L7 or anti-L1. Fig. 3*A* shows that L1 was secreted into the medium only when L7 was co-expressed. Cholesterol and epicholesterol did not affect this secretion (Fig. 3*A*, *lanes 12–14*). In another experiment, we delivered cholesterol with β-VLDL, a cholesterol-carrying lipoprotein that binds to LDL receptors. Secretion was not affected by β-VLDL even when supplemented with cholesterol complexed to MCD (Fig. 3*B*, *lanes 12–14*).

To facilitate further studies of the L1-L7 complex, we shifted to the baculovirus expression system in insect cells to produce large quantities of L1-L7 protein. The baculoviruses used for experiments in Fig. 4 encoded L1, L7, and L1-L7, each of which was preceded by a cassette composed of the signal sequence from honeybee mellitin followed by six histidines (L1) or 10 histidines (L7 and L1-L7). As with the mammalian L1-L7 fusion protein, the baculovirus fusion L1-L7 protein contained a 15-amino acid linker containing a TEV cleavage site that separated L1 from L7 (Fig. 2*D*).

When expressed alone in the insect cells, all L1 was retained in the cells (Fig. 4*A*, *lanes 3* and *4*), whereas a significant fraction of L7 (~35% of total) was secreted into the medium (Fig. 4*A*, *lanes 7* and *8*). L1-L7 was also largely retained in cells, but a significant fraction (~15% of total) was secreted into the medium (Fig. 4*A*, *lanes 11* and *12*). Note that 20-fold higher aliquots of medium (Fig. 4*A*, *lanes 4*, *8*, and *12*) relative to cell lysates (Fig. 4*A*, *lanes 3*, *7*, and *11*) were loaded onto these gels (see legend for Fig. 4). When subjected to $10^5 \times g$ centrifugation, cell-retained L1, L7, and L1-L7 were found in the membrane pellet (Fig. 4*B*, *lanes 1*, *2*, *5*, *6*, *9*, and *10*), and all could be solubilized by treatment with FC13 detergent (Fig. 4*B*, *lanes 3*, *4*, *7*, *8*, *11*, and *12*). Secreted L7 was equally distributed between the soluble supernatant and insoluble pellet fractions after a $10^5 \times g$ centrifugation step and could be completely solubilized by FC13 (Fig. 4*C*, *lanes 1–4*). In contrast, all of the secreted L1-L7 was soluble even in the absence of FC-13 (Fig. 4*C*, *lanes 5–8*).

We purified the secreted soluble L1-L7 by nickel chromatography followed by gel filtration, both performed in the absence of detergents (Fig. 5). Gel filtration showed that L1-L7 elutes as a single, sharp peak corresponding to an apparent molecular mass of 72 kDa, somewhat higher than the calculated molecular

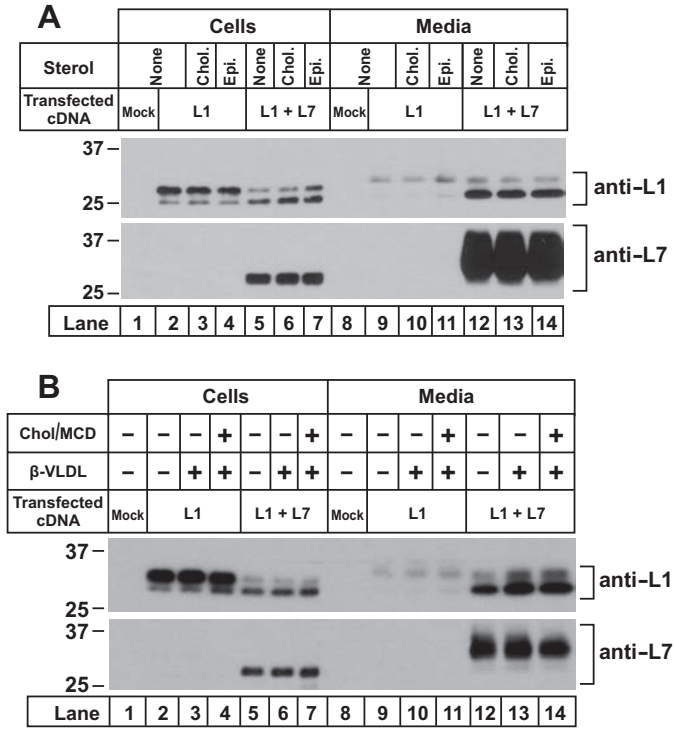

FIGURE 3. **L7-mediated secretion of L1 by CHO-K1 cells is not affected by treatment with sterol-cyclodextrin complexes or β-VLDL.** *A* and *B*, on day 0, CHO-K1 cells were set up for experiments in 3 ml of medium A containing 5% FCS at a density of 6×10^5 cells/60-mm dish. On day 1, cells were switched to 3 ml of medium A containing 1% ITS and co-transfected with either 2 μg of pCMV-Scap-L1 or 2 μg of pCMV-Scap-L1 plus 2 μg of pCMV-Scap-L7. FuGENE 6 was used as the transfection agent according to the instructions of the manufacturer. The total amount of DNA was adjusted to 4 μg/dish by addition of pcDNA empty vector. *A*, on day 3, cells were switched to 3 ml of medium A containing 50 μM of the indicated sterol-MCD complex. After 6 h, medium was collected from each group (2 dishes/condition) and pooled (6 ml total), and the cells from each group were harvested, pooled, and resuspended in PBS (1 ml total). *B*, on day 2, cells were switched to 3 ml of medium A containing 1 μg/ml β-VLDL without or with 50 μM cholesterol-MCD complexes. On day 3, medium was collected from each group (2 dishes/condition) and pooled (6 ml total), and the cells from each group were harvested, pooled, and resuspended in PBS (1 ml total). *A* and *B*, equivalent fractions of cells and medium (0.6% of total) were then subjected to immunoblot analysis with 5 μg/ml anti-L1 or 0.5 μg/ml anti-L7. *Chol*, cholesterol; *Epi*, epicholesterol.

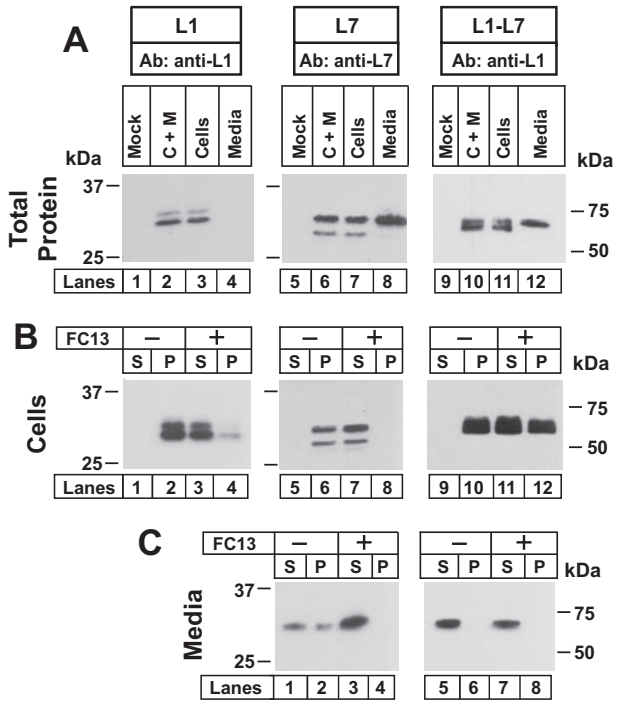

FIGURE 4. **Secretion of soluble His_{10}-Scap(L1-L7) by Sf9 insect cells.** *A*, comparison of localization of His_6-Scap-L1, His_{10}-Scap-L7, and His_{10}-Scap(L1-L7). Sf9 cells were infected with the indicated Scap baculovirus as described under "Experimental Procedures." To measure secretion into the medium, 80 μl of baculovirus-infected Sf9 cell suspension (representing $\sim 6 \times 10^5$ cells) was centrifuged at 4000 $\times$ *g* for 5 min at room temperature, after which the resulting pellets were solubilized in 1.6 ml of buffer B. Equal aliquots of the original cell suspension (*C* + *M*) and solubilized cell pellets (*Cells*) (1.25% of total) and 20-fold higher aliquots of the supernatants (*Media*) (25% of total), were subjected to 13% SDS-PAGE and immunoblot analysis with 5 μg/ml anti-L1 or 1 μg/ml anti-L7. *B* and *C*, solubility of Scap proteins. In a total volume of 100 μl, aliquots (5% of total) of cells and medium from *A* were incubated with 1% (w/v) FC13 detergent for 1 h, centrifuged at $10^5 \times g$ for 1 h, and the resulting supernatants (*S*) and pellets (*P*) were subjected to immunoblot analysis as described above.

mass of 53 kDa (Fig. 5*A*, *top panel*). Immunoblot analysis confirmed that the eluted peak fractions contained L7 (Fig. 5*A*, *bottom panel*). The purified L1-L7 migrated as a single band on SDS/PAGE, as visualized by Coomassie Blue staining (Fig. 5*B*). The band was also visualized with antibodies against either L1 or L7 (Fig. 5*B*). Treatment of L1-L7 with PNGase F reduced its apparent molecular weight (Fig. 5*B*), indicating that at least one of its N*X*S or N*X*T sequences had been glycosylated.

We used the soluble, detergent-free L1-L7 purified from Sf9 medium for cholesterol binding studies. To measure binding, we incubated L1-L7 with [^{3}H]cholesterol in buffer containing 0.004% NP40 and 0.002% FC13. Even though L1-L7 does not require detergents for solubility, we included submicellar concentrations of NP40 and FC13 to prevent precipitation of the hydrophobic sterol ligands. The reaction mixture was applied to a nickel column, washed with detergent-free buffers, and protein-bound [^{3}H]cholesterol was eluted with 250 mM imidazole in detergent-free buffer for quantification by scintillation counting. As shown in Fig. 5*C*, L1-L7 bound [^{3}H]cholesterol with saturation kinetics and showed a slightly lower affinity (calculated K_d, $\sim$150 nM) compared with reported K_d values of 50–100 nM for detergent-solubilized L1 (6) and the entire membrane domain of Scap solubilized in detergent (15). To analyze the sterol specificity of L1-L7 binding, we performed competition studies with various unlabeled sterols. Desmosterol competed as well as cholesterol for [^{3}H]cholesterol binding, whereas epicholesterol and 25-hydroxycholesterol showed a much lower affinity (Fig. 5*D*). This sterol specificity is the same as that reported earlier for detergent-solubilized L1 and the membrane domain of Scap (6, 9).

We also tested the secretion by insect cells of L1-L7 containing mutations (Y234A in L1 and Y640S in L7) that have been shown previously to disrupt the binding of L1 to L7 (6, 7). As shown in Fig. 6*A*, when we infected insect cells with these L1-L7 baculoviruses, we observed secretion of WT L1-L7 ($\sim$15% of total) but no detectable secretion of the Y640S or Y234A mutants of L1-L7. When we infected insect cells with a baculovirus encoding L7 alone harboring the Y640S mutation, its secretion was similar to that of WT L7 (Fig. 6*B*), indicating that this mutant L7 was not misfolded. Moreover, we showed previously that L1 harboring the Y234A mutation bound [^{3}H]cholesterol with a similar affinity as WT L1 (6), indicating that this mutant L1 was not misfolded.

Fig. 7 shows an experiment designed to determine whether L1 and L7 would remain associated in the presence of cholesterol. To perform cholesterol incubations, we first determined detergent conditions that would preserve the L1-L7 interaction after cleavage of the linker with TEV protease. After TEV treatment, the proteins were incubated in the absence or presence of various detergents and then immunoprecipitated with anti-L1 (Fig. 7*A*), subjected to SDS-PAGE, and blotted with anti-L1 or anti-L7 (Fig. 7*B*). In the absence of detergent, both L1 and L7 were found in the pellet, indicating that the complex remained intact (Fig. 7*B*, *lanes 1* and *6*). The presence of NP40 or CHAPS had no effect (Fig. 7*B*, *lanes 3*, *4*, *8*, and *9*). However, the addition of FC13 or octylglucoside disrupted the complex so that L7 remained in the supernatant after precipitation with anti-L1 (Fig. 7*B*, *lanes 2*, *5*, *7*, and *10*). We then tested whether L1 and L7 could be dissociated by cholesterol treatment in the presence of NP40 or CHAPS, which do not themselves disrupt the complex. After treatment with TEV protease, the complex was incubated in the presence of NP40 or CHAPS without or with cholesterol solubilized in ethanol. The complexes were then immunoprecipitated with anti-L1 or a control antibody (Fig. 7*C*). In the absence of cholesterol, L1 and L7 remained in a complex after their TEV linker was cleaved (Fig. 7*C*, *lanes 2*, *4*, *7*, and *9*). Incubation with 5 μM cholesterol for 5 h did not dissociate L1 from L7 (Fig. 7*C*, *lanes 1–10*).

Discussion

This paper provides important insights into the mechanism by which a membrane protein, *i.e.* Scap, can sense the level of a membrane lipid, *i.e.* cholesterol, and orchestrate a homeostatic response. Previous studies have led us to focus on the two large luminal loops of Scap, L1 and L7 (6, 7). In the earlier studies, we first found that L1 binds cholesterol with a specificity that matches the binding activity of the whole protein (6). Then we used transfection to express a portion of Scap extending from the NH_2 terminus to the middle of cytosolic Loop6. In the same cells, we expressed the remaining portion of Scap extending from Loop6 to the COOH terminus (7). We found that these

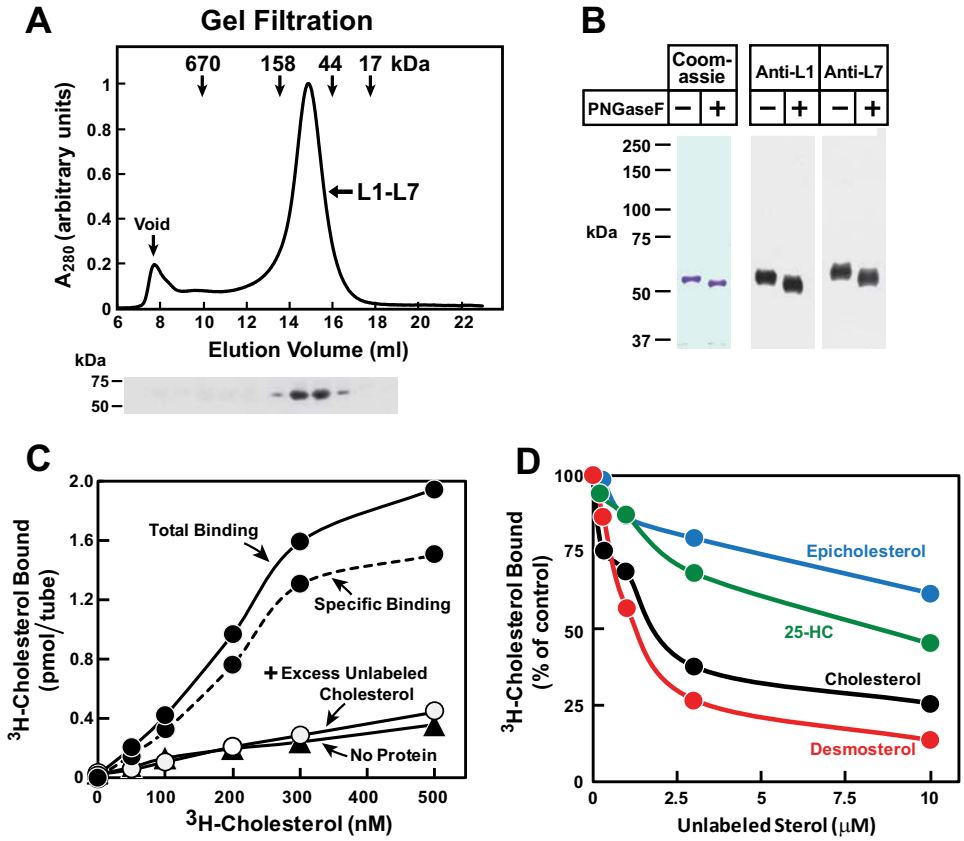

FIGURE 5. **Biochemical characterization of His_{10}-Scap(L1-L7) purified from Sf9 cells.** *A*, gel filtration chromatography. Recombinant His_{10}-Scap(L1-L7) was isolated by nickel chromatography from the culture medium of Sf9 cells as described under "Experimental Procedures." Buffer A (500 μl) containing 1.4 mg of His_{10}-Scap(L1-L7) was loaded onto a Superdex 200 10/300 column and chromatographed at a flow rate of 0.5 ml/min. Fractions of 1 ml each were collected. Absorbance at 280 nm was monitored continuously to identify His_{10}-Scap(L1-L7) (*top panel*). Standard molecular weight markers (thyroglobulin, M_r 670,000; γ-globulin, M_r 158,000; ovalbumin, M_r 44,000; and myoglobin, M_r 17,000) were chromatographed on the same column under identical buffer conditions (*arrows*). The apparent molecular mass for His_{10}-Scap(L1-L7) is 72 kDa. Aliquots of each fraction (20 μl) were subjected to 13% SDS-PAGE and immunoblot analysis with 0.15 μg/ml anti-L7 (*bottom panel*). Fractions eluting between 13 and 17 ml that contained the peak A_{280} activity were pooled and concentrated. *B*, an aliquot of the pooled fractions (200 μg) was incubated with 6 μl of PNGase F (3000 units) at room temperature for 2 h. The untreated and PNGase F-treated samples were then subjected to 8% SDS-PAGE, and His_{10}-Scap(L1-L7) was detected by staining with Coomassie Brilliant Blue R-250 (2 μg/lane) or by immunoblot analysis (80 ng/lane) with 0.13 μg/ml anti-L1 or 1 μg/ml anti-L7. *C*, saturation binding of [^{3}H]cholesterol to purified His_{10}-Scap(L1-L7). Each reaction, in a final volume of 100 μl of buffer A with 0.004% (w/v) NP40 and 0.002% (w/v) FC13, contained 2 pmol of purified His_{10}-Scap(L1-L7) and the indicated concentration of [^{3}H]cholesterol (111,000 dpm/pmol) in the absence or presence of 10 μM unlabeled cholesterol, as indicated. After 4 h at room temperature, the bound [^{3}H]cholesterol was measured by nickel chromatography as described under "Experimental Procedures." Each data point denotes the average of duplicate assays. Specific [^{3}H]cholesterol binding is total binding after subtraction of blank values determined in the presence of the unlabeled cholesterol at 10 μM (<0.36 pmol/tube). *D*, competition for binding of [^{3}H]cholesterol to His_{10}-Scap(L1-L7). Each reaction, in a final volume of 100 μl of buffer A with 0.004% (w/v) NP40 and 0.002% (w/v) FC13, contained 4 pmol of His_{10}-Scap(L1-L7), 150 nM [^{3}H]cholesterol (111,000 dpm/pmol) and varying concentrations of the indicated unlabeled sterol. After 4 h at room temperature, bound [^{3}H]cholesterol was measured as above. Each value represents total binding without subtraction of blank values and is the average of duplicate assays. The "100% of control" values, determined in the absence of unlabeled sterols, was 1.1 pmol/tube. *25-HC*, 25-hydroxycholesterol.

two halves of Scap formed a complex in ER membranes, as revealed by co-immunoprecipitation. Complex formation was abrogated by point mutations in L1(Y234A) or L7(Y640S). We interpreted this result to indicate that the two halves of the protein were held together by direct binding of L1 to L7 and that the point mutations prevented this binding. When introduced into full-length Scap, these point mutations prevented the Scap-SREBP complex from moving to the Golgi, thus mimicking Scap in the cholesterol-bound conformation (6, 7). These results allowed us to advance the hypothesis that cholesterol binding to L1 causes it to dissociate from L7 and that this dissociation prevents the binding of COPII proteins to the MELADL sequence in Loop6. The conformational change is assisted by the binding of Insig to the region between transmembrane helices 2 and 6 (Fig. 1).

The current data support part of this hypothesis by demonstrating directly that L1 binds to L7. Binding occurred when the two loops were expressed jointly and independently of the rest of Scap. When expressed alone, L1 remained firmly attached to cell membranes and required detergents for solubilization (Fig. 4 and Ref. 6). When L1 and L7 were co-expressed as individual molecules, L1 formed a soluble complex with L7 that was secreted into the medium. This complex could be immunoprecipitated with an antibody to L7 (Fig. 2*C*). When expressed as an L1-L7 fusion protein, L1-L7 was secreted into the medium as a soluble species that behaved as a discrete protein on gel filtration (Fig. 5*A*). The L1-L7 fusion protein retained the ability to bind cholesterol (Fig. 5, *C* and *D*), an observation that confirms that L1 was in its native configuration. Moreover, the complex failed to be secreted when L1

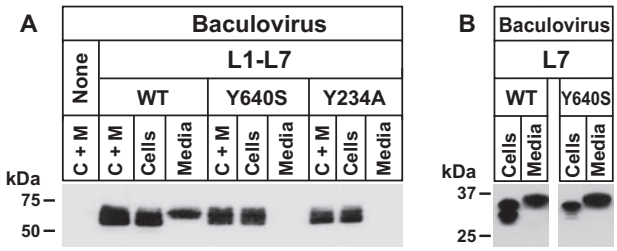

FIGURE 6. **Secretion of soluble His_{10}-Scap(L1-L7) by Sf9 insect cells is blocked by mutations that disrupt the interaction between L1 and L7.** *A* and *B*, Sf9 cells were infected with a baculovirus encoding the indicated versions of His_{10}-Scap(L1-L7) (*A*) or His_{10}-Scap-L7 (*B*) as described under "Experimental Procedures." To measure secretion into the medium, 80 μl of baculovirus-infected Sf9 cell suspension (representing $\sim 6 \times 10^5$ cells) were centrifuged at 4000 $\times$ *g* for 5 min at room temperature, after which the resulting pellets were solubilized in 1.6 ml of buffer B. *A*, equal aliquots of the original cell suspension (*C* + *M*) and solubilized cell pellets (*Cells*) (1.25% of total), and 20-fold higher aliquots of the supernatants (*Media*) (25% of total) were subjected to 13% SDS-PAGE and immunoblot analysis with 5 μg/ml anti-L7. *B*, aliquots of solubilized cell pellets (*Cells*) (1.25% of total) and 20-fold higher aliquots of the supernatants (*Media*) (25% of total) were subjected to 13% SDS-PAGE and immunoblot analysis with a 1:5000 dilution of anti-His antibody.

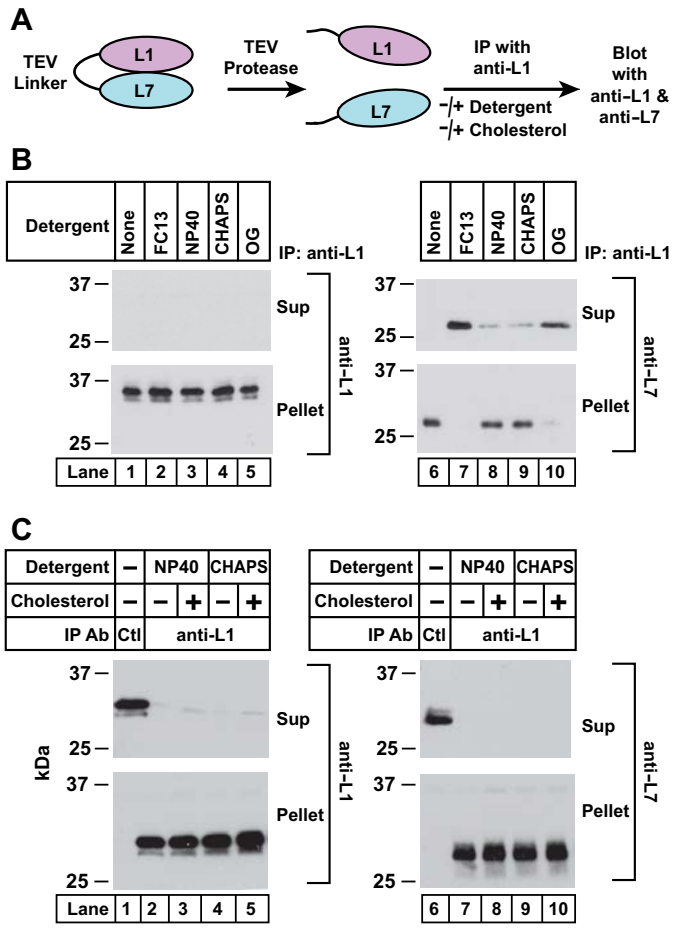

FIGURE 7. **Co-immunoprecipitation of L1 and L7 after proteolytic release from purified His_{10}-Scap(L1-L7) fusion protein.** *A*, schematic of the assay for the interaction between L1 and L7. *IP*, immunoprecipitation. *B* and *C*, co-immunoprecipitation of L1 and L7. Initial reactions, either in a final volume of 350 μl of buffer A containing 500 pmol of purified His_{10}-Scap(L1-L7) and 50 units of TEV protease (*B*) or in a final volume of 520 μl of buffer A containing 1000 pmol of purified His_{10}-Scap(L1-L7) and 200 units of TEV protease (*C*) were incubated overnight at 4 °C. *B*, after the overnight cleavage reaction, further reactions were set up, each in a final volume of 200 μl of buffer A containing 50 pmol of cleaved His_{10}-Scap(L1-L7) and 0.1% (w/v) FC13, 0.1% (w/v) NP40, 1% (w/v) CHAPS, or 1% (w/v) octylglucoside (*OG*), as indicated. After incubation for 2 h at room temperature, 400 μl of buffer A was added to each reaction. *C*, after the overnight cleavage reaction (see above), further reactions were set up, each in a final volume of 200 μl of buffer A containing 10 pmol of cleaved His_{10}-Scap(L1-L7) and either 0.1% NP40 or 1% CHAPS without or with 5 μM cholesterol (added in 5 μl ethanol), as indicated. After incubation for 5 h at room temperature, 400 μl of buffer A was added to each reaction. *B* and *C*, reaction mixtures were then subjected to immunoprecipitation with 1 μg/ml anti-L1, as described under "Experimental Procedures." Equivalent fractions of pellets and supernatants (*Sup*) (each 2% of total) were subjected to immunoblot analysis with either 5 μg/ml anti-L1 or 5 μg/ml anti-L7. *Ctl*, control.

contained the Y234A mutation or L7 contained the Y640S mutation (Fig. 6). These two mutations were shown previously to prevent the association of the two halves of Scap in intact cells (6, 7). All of these findings support the idea that the binding of isolated L1 to L7 mimics the interaction between these loops that occurs in the whole protein.

The second part of the hypothesis, namely, that cholesterol binding dissociates L1 from L7, remains unproven. Despite many efforts, we have been unable to show that cholesterol prevents the association of isolated L1 with L7 in cells (Fig. 3) or in the context of the L1-L7 fusion protein (Fig. 7*C*). It is likely that this dissociation requires a conformational change in the five transmembrane helices that separate L1 from L7 (Fig. 1). Studies to document such a conformational change are underway.

An interesting finding in this study relates to glycosylation. When full-length Scap is expressed, the *N*-linked glycosylation site in L1 (NCS) is glycosylated (8). As shown in Fig. 2*B*, when L1 was expressed alone, the protein was membrane-bound, and it was glycosylated as revealed by PNGase F digestion. When L7 was co-expressed, L1 was not glycosylated, even when it was secreted into the medium. *N*-linked glycosylation is thought to occur co-translationally. It is noteworthy that the NCS sequence is near the COOH terminus of L1 and that it is not translated until the bulk of L1 has been translated and the protein has folded, at least partially. The data suggest that excess free L7 binds to the partially folded L1 and blocks access of the glycosyltransferases. A different result was observed when L7 followed L1 in the L1-L7 fusion construct. In this case, L7 is not synthesized until L1 has been completely translated and glycosylated. As a result, in the context of the fusion protein, L1 was glycosylated (Fig. 2*E*). Similarly, in full-length Scap, L7 is not translated until after L1 has been translated and glycosylated.

Considered together with previous data, this paper brings us closer to a molecular understanding of the mechanism by which a membrane protein, Scap, can detect and respond to the concentration of a membrane lipid, cholesterol. Further understanding will come from a combination of biochemical analysis and structural information. It is possible that these studies will expose a general mechanism by which membrane proteins can detect and regulate membrane lipids.

Author Contributions—Y. Z., K. M. L., and L. C. designed, performed, and analyzed the experiments. L. N. K., N. V. G., and D. M. R. designed the experiments. M. S. B., J. L. G., and A. R. designed the research, analyzed the data, and wrote the paper. All authors reviewed the results and approved the final version of the manuscript.

Acknowledgments—We thank Linda Donnelly and Angela Carroll for producing the anti-L1 antibody; Lisa Beatty, Hue Dao, Shomanike Head, Ijeoma Dukes, and Lucie Batte for help with tissue culture; and Daphne Rye, Dorothy Williams, and Donna Frias for technical assistance.

References

1. Brown, M. S., and Goldstein, J. L. (2009) Cholesterol feedback: from Schoenheimer's bottle to Scap's MELADL. *J. Lipid Res.* **50,** S15-S27
2. Brown, M. S., and Goldstein, J. L. (1997) The SREBP pathway: regulation of cholesterol metabolism by proteolysis of a membrane-bound transcription factor. *Cell* **89,** 331–340
3. Horton, J. D., Goldstein, J. L., and Brown, M. S. (2002) SREBPs: activators of the complete program of cholesterol and fatty acid synthesis in the liver. *J. Clin. Invest.* **109,** 1125–1131
4. Radhakrishnan, A., Goldstein, J. L., McDonald, J. G., and Brown, M. S. (2008) Switch-like control of SREBP-2 transport triggered by small changes in ER cholesterol: a delicate balance. *Cell Metab.* **8,** 512–521
5. Sun, L.-P., Li, L., Goldstein, J. L., and Brown, M. S. (2005) Insig required for sterol-mediated inhibition of Scap/SREBP binding to COPII proteins *in vitro*. *J. Biol. Chem.* **280,** 26483–26490
6. Motamed, M., Zhang, Y., Wang, M. L., Seemann, J., Kwon, H. J., Goldstein, J. L., and Brown, M. S. (2011) Identification of luminal Loop 1 of Scap protein as the sterol sensor that maintains cholesterol homeostasis. *J. Biol. Chem.* **286,** 18002–18012
7. Zhang, Y., Motamed, M., Seemann, J., Brown, M. S., and Goldstein, J. L. (2013) Point mutation in luminal Loop 7 of Scap blocks interaction with Loop 1 and abolishes movement to Golgi. *J. Biol. Chem.* **288,** 14059–14067
8. Nohturfft, A., Brown, M. S., and Goldstein, J. L. (1998) Topology of SREBP cleavage-activating protein, a polytopic membrane protein with a sterol-sensing domain. *J. Biol. Chem.* **273,** 17243–17250
9. Radhakrishnan, A., Ikeda, Y., Kwon, H. J., Brown, M. S., and Goldstein, J. L. (2007) Sterol-regulated transport of SREBPs from endoplasmic reticulum to Golgi: oxysterols block transport by binding to Insig. *Proc. Natl. Acad. Sci. U.S.A.* **104,** 6511–6518
10. Sun, L.-P., Seemann, J., Brown, M. S., and Goldstein, J. L. (2007) Sterol-regulated transport of SREBPs from endoplasmic reticulum to Golgi: Insig renders sorting signal in Scap inaccessible to COPII proteins. *Proc. Natl. Acad. Sci. U.S.A.* **104,** 6519–6526
11. Kovanen, P. T., Brown, M. S., Basu, S. K., Bilheimer, D. W., and Goldstein, J. L. (1981) Saturation and suppression of hepatic lipoprotein receptors: a mechanism for the hypercholesterolemia of cholesterol-fed rabbits. *Proc. Natl. Acad. Sci. U.S.A.* **78,** 1396–1400
12. Sakai, J., Nohturfft, A., Cheng, D., Ho, Y. K., Brown, M. S., and Goldstein, J. L. (1997) Identification of complexes between the COOH-terminal domains of sterol regulatory element-binding proteins (SREBPs) and SREBP cleavage-activating protein (SCAP). *J. Biol. Chem.* **272,** 20213–20221
13. Loftus, S. K., Morris, J. A., Carstea, E. D., Gu, J. Z., Cummings, C., Brown, A., Ellison, J., Ohno, K., Rosenfeld, M. A., Tagle, D. A., Pentchev, P. G., and Pavan, W. J. (1997) Murine model of Niemann-Pick C disease: mutation in a cholesterol homeostasis gene. *Science* **277,** 232–235
14. Kapust, R. B., Tözsér, J., Copeland, T. D., and Waugh, D. S. (2002) The P1′ specificity of tobacco etch virus protease. *Biochem. Biophys. Res. Comm.* **294,** 949–955
15. Radhakrishnan, A., Sun, L.-P., Kwon, H. J., Brown, M. S., and Goldstein, J. L. (2004) Direct binding of cholesterol to the purified membrane region of SCAP: mechanism for a sterol-sensing domain. *Mol. Cell* **15,** 259–268
16. Brown, A. J., Sun, L., Feramisco, J. D., Brown, M. S., and Goldstein, J. L. (2002) Cholesterol addition to ER membranes alters conformation of SCAP, the SREBP escort protein that regulates cholesterol metabolism. *Mol. Cell* **10,** 237–245